



Numerically efficient full-vectorial rational Chebyshev pseudo-spectral modal analysis for optical Waveguides

Afaf Said¹ · Salah Obayya¹

Received: 10 May 2023 / Accepted: 5 August 2023 / Published online: 20 September 2023
© The Author(s) 2023

Abstract

In this paper, an efficient full-vectorial modal analysis based on the rational Chebyshev pseudo-spectral method (V-RCPSM) is introduced to analyze 3 dimensional (3D) structures that are invariant along one spatial variable. Such structures are essential in silicon photonics and plasmonics applications where permittivity profiles with high-index contrast need precise treatment of the interface boundary conditions. Besides, such structures are open in general. Hence, good domain truncation is important. Our method handles these challenges via hybrid usage of the domain decomposition technique where the electromagnetic field is expanded in terms of Chebyshev functions in homogeneous regions, while the rational Chebyshev functions are used for semi-infinite homogeneous domains. The boundary conditions are rigorously imposed along the interfaces, a step that maintains the known exponential convergence rate of Chebyshev functions. Chebyshev functions have the ability to capture the correct rapid variation of the electromagnetic fields at the interfaces of the high-index-contrast waveguides using only a few basis functions; a critical feature for accurate mode computation. To show the accuracy and efficiency of our new approach, we studied rib and plasmonic waveguides and compared the results with those obtained using other full-vectorial approaches such as the finite elements method (FEM). Our developed approach has achieved a huge reduction in computational resources over the FEM.

Keywords Plasmonics · High-index-contrast waveguide · Full-vectorial modal analysis · Rational Chebyshev pseudo-spectral method

1 Introduction

Silicon photonics is well known for becoming a leading technology in photonics enabling many devices in sub-wavelength dimensions. Plasmonics, as another promising branch of photonics, is playing a vital role in the realization of many devices and systems beyond

✉ Salah Obayya
sobayya@zewailcity.edu.eg

Afaf Said
asaaid@zewailcity.edu.eg

¹ Center for Photonics and Smart Materials (CPSM), Zewail City of Science and Technology, Ahmed Zewail Road, October Gardens, 6th of October City 12578, Giza, Egypt

the diffraction limit penetrating a wide range of applications such as integrated optics (Maier 2006), communications (Carvalho et al. 2020), high-sensitive sensing (Lee et al. 2021; Azzam et al. 2016), biomedical applications (Gamal et al. 2022), and others (Said et al. 2020). Also, plasmonics shows promise to merge photonics in its big sub-wavelength dimensions to electronics at the nanoscale for optoelectronic chips (Ozbay 2006; Atia et al. 2019). Optical waveguides are the key component of such photonic devices and optoelectronic chips. Both silicon photonics and plasmonics produce high-index contrast structures showing rapid variation in the fields at the interfaces between the silicon or the metal and the surrounding dielectric material. Thus, solving such high field values requires huge computational resources. Therefore, the efficient modeling techniques of such basic components, waveguides, are still a challenge and need much more considerable effort to correctly represent the light-matter interaction at such high-index contrast interfaces (Said et al. 2020).

The accuracy of the finite elements method (FEM) (Koshiba et al. 1982; Obayya et al. 2003; Said et al. 2020) and the finite difference method (FDM) (Lusse et al. 1994; Said et al. 2020) depends on the mesh. Moreover, nonphysical domain truncation techniques to represent infinite or semi-infinite computational domains are required. Perfectly matched layers (PMLs), or variants of transparent boundary conditions, are commonly conventional approaches that cause some numerical problems (Said et al. 2020). However, FEM based on “Master” and “Slave” nodes requires a considerable amount of logic for coupling the related degrees of freedom and does not easily lend itself to developing programs as extensions to existing general-purpose finite-element packages. Moreover, FEM based on “edge elements” of leaving the normal component of the expanded function free to jump across common faces of adjacent elements was shown to be a possible source of spurious surface charges on those faces and led to nonsymmetric systems of linear, algebraic equations and may lead to singularity (Lager and Mur 1998). In addition, these edge elements-based technique is computationally more expensive in terms of both storage requirements and efficiency of iterative solvers. Otherwise, the superposition of an auxiliary continuous function on linear nodal elements results in lower accuracy (Koshiba and Tsuji 2000). All these problems suggest the need for a new type of vectorial expansion function that combines the regularity properties of the nodal elements with the capability of modeling the behavior of the field strength across interfaces.

Alternatively, spectral methods and conformal maps are introduced as semi-analytical methods based on global basis functions to represent semi-infinite or infinite domains, eliminating the need for PMLs, by Laguerre or Hermite basis functions and others (Abdrabou et al. 2016). These techniques achieve faster convergence than conventional mesh-based methods (Said et al. 2020). The pseudo-spectral methods have the ability to properly apply the physical boundary conditions at the interfaces of the discontinuity between metal and dielectric materials. However, only 1D solver based on the pseudo-spectral method (Abdrabou et al. 2016) has been introduced for the accurate modal analysis of dielectric and plasmonic waveguides. Although pseudo-spectral methods have been successfully adopted for the accurate and fast modal analysis of dielectric waveguides (Huang 2010; Huang et al. 2005), they have never been used for 2D full-vectorial modal analysis of plasmonic waveguides or other high-index contrast devices like in silicon photonics.

In this paper, we introduce a 2D full-Vectorial modal analysis based on the rational Chebyshev Pseudo-spectral Method (V-RCPSM) to achieve high accuracy for high-index contrast waveguides with a reduction in computational resources. The efficiency and accuracy of V-RCPSM have been proven through the analysis of a rib waveguide and a plasmonic waveguide, the results have been compared with another full-vectorial modal solver, full

vector finite-element method (Obayya et al. 2002). This is the first time, to the best of our knowledge, to develop such a technique, V-RCPSM, for the 2D full-vectorial modal analysis of the challenging high-index contrast waveguides like in silicon photonics and plasmonics. The paper is organized as follows: Sect. 2 presents V-RCPSM, the pseudospectral approach for the full-vectorial modal analysis based on the rational Chebyshev functions with Algebraic maps; Sect. 3 presents two examples to demonstrate the computational performances in convergence and accuracy of the proposed method; Sect. 4 draws the conclusions.

2 Full-vectorial modal analysis based on the rational Chebyshev pseudo-spectral method (V-RCPSM)

In the pseudo-spectral approach (Huang et al. 2005; Huang 2010) for the modal analysis of the transverse cross-section of the 3D waveguide shown in Fig. 1a, the computational domain, in the x-y plane, is divided into several finite and semi-infinite subdomains with uniform or continuous refractive index profiles as shown in Fig. 1b. To calculate the modes of the waveguide in Fig. 1b, we start from Maxwell’s equations in the frequency domain to obtain the vector wave equation for the magnetic field vector, H , as follows,

$$\nabla^2 H + k_0^2 n^2 H + \frac{\nabla n^2}{n^2} (\nabla \times H) = 0, \tag{1}$$

where n is the refractive index profile of the waveguide, and k is the wavenumber. For the full-vectorial 2D modal analysis, all electromagnetic fields are assumed to have a z

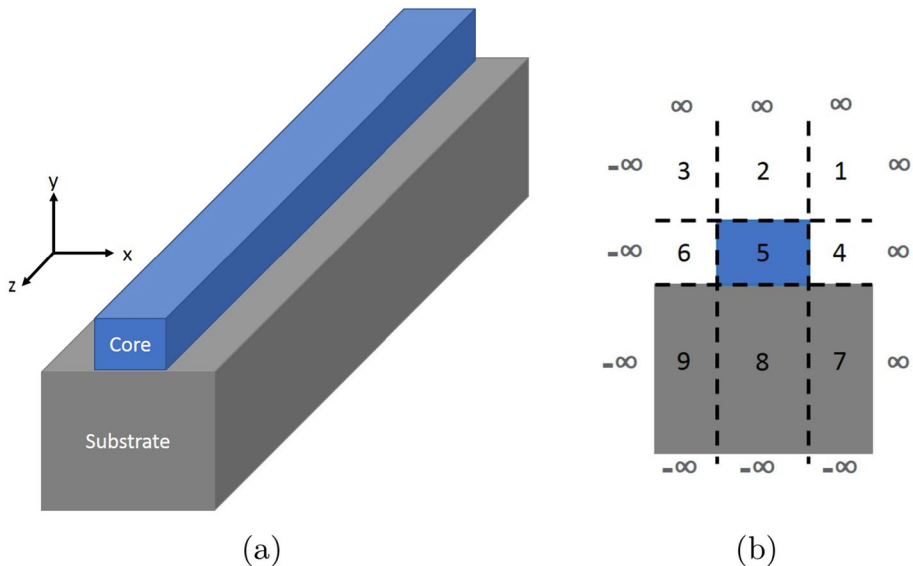


Fig. 1 (a) Schematic for a 3D structure targeted to be analyzed by the 2D modal solver based on the Chebyshev pseudo-spectral method. (b) The 2D cross-section of the waveguide using the spectral method to divide the structure into subdomains: finite and semi-infinite subdomains

dependence of $e^{-j\beta z}$, then the continuity of the longitudinal components H_z and E_z can incorporate the coupled relations of H_x and H_y (Huang et al. 2005; Huang 2010). The two coupled components of the magnetic fields, H_x, H_y , are derived as,

$$\nabla^2 H_x + k_0^2(n^2 - n_{eff}^2)H_x - \frac{1}{n^2} \frac{\partial n^2}{\partial y} \frac{\partial H_x}{\partial y} + \frac{1}{n^2} \frac{\partial n^2}{\partial y} \frac{\partial H_y}{\partial x} = 0, \tag{2}$$

$$\nabla^2 H_y + k_0^2(n^2 - n_{eff}^2)H_y - \frac{1}{n^2} \frac{\partial n^2}{\partial x} \frac{\partial H_y}{\partial x} + \frac{1}{n^2} \frac{\partial n^2}{\partial x} \frac{\partial H_x}{\partial y} = 0, \tag{3}$$

where $n_{eff} = \beta/k_0$ is the effective index of the waveguide mode, and β is the propagation constant.

2.1 Rational Chebyshev functions with algebraic maps

We now determine the appropriate basis functions by expanding the H_x and H_y components using the Chebyshev polynomials which are regarded as a better technique for expanding the optical fields in interior subdomains because of their mathematical robustness to non-periodic structures. The proposed method is based on the cardinal Chebyshev function first introduced for 1D modal analysis in Abdrabou et al. (2016), and here we extend the method for the 2D full-vectorial modal analysis (V-RCPSM) to solve the system of Eqs. 2 and 3. The magnetic field components, H_x and H_y , are obtained by expanding the field in terms of mapped basis functions obtained by composing Chebyshev functions $S_{i,j}(l)$ by the suitable conformal map for each subdomain (Abdrabou et al. 2016), the field expansion and its grid values in a subdomain at the collocation points take the form

$$H_l = \sum_{i=-M}^N \sum_{j=-M}^N u_{ij}^{(l)} S_i(x) S_j(y), l = x, y. \tag{4}$$

The system of differential Eqs. 2 and 3 is thus converted to an algebraic eigenvalue problem.

$$\begin{bmatrix} A_{xx} & A_{xy} \\ A_{yx} & A_{yy} \end{bmatrix} \begin{Bmatrix} vec(u_{ij}^x) \\ vec(u_{ij}^y) \end{Bmatrix} = \beta^2 \begin{Bmatrix} vec(u_{ij}^x) \\ vec(u_{ij}^y) \end{Bmatrix} \tag{5}$$

where $vec(\cdot)$ is a vectorization operator and the matrices A_{xx}, A_{xy}, A_{yx} and A_{yy} are the differentiation matrices of the operators in Eqs. 2 and 3.

We adopt the linear maps (Abdrabou et al. 2016) for the 2D bounded subdomains. We apply the Dirichlet zero boundary condition (BC) at the infinity, x or $y = \pm\infty$, and extend the algebraic maps (Abdrabou et al. 2016) for the 2D semi-infinite subdomains.

We expand the basis functions for each dimension individually. So, the conformal mappings are still 1D not 2D. For instance, if we suppose that the x direction extends to infinity, we map it with 1D conformal mapping like what is exactly used in Abdrabou et al. (2016). Other finite dimensions can be mapped by linear maps. So, mapping the 2D structures here is not 2D, it is by independent 1D maps, just like the cross product or set product of two 1D maps: conformal and/or linear maps, exactly as the same 1D maps in the previous paper (Abdrabou et al. 2016), but applied in each dimension separately.

Fig. 2 RIB waveguide 2D cross-section

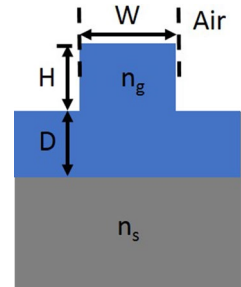


Table 1 Effective index (n_{eff}) for the rib waveguide, shown in the previous figure, for different values of D computed by our new full vectorial spectral method, V-RCPSM, (Present) and full vectorial finite element method (VFEM) reported in Obayya et al. (2002)

D (μm)	V-RCPSM (Present)	VFEM, Ref (Obayya et al. 2002)
0.1	3.412133	3.41213
0.2	3.412288	3.41229
0.3	3.412502	3.41250
0.4	3.412786	3.41279
0.5	3.413145	3.41314
0.6	3.413584	3.41358
0.7	3.414114	3.41410
0.8	3.414761	3.41373
0.9	3.415598	3.41558

Moreover, since we use an H formula, the magnetic field is zero outside. We are applying an infinite domain at the boundary of our physical domain, and then we truncate with Dirichlet BC at infinity. This means no matter what material we are using the field will smoothly decay in the infinite domain mimicking the field leaving our physical domain. The Dirichlet BC here will not cause any reflections since it is placed at infinity. Moreover, for other physical cases at the boundaries, other BC can be easily integrated with our V-RCPSM approach.

Extra details about the mathematical derivation for the full-vectorial H formulation, the conformal mapping, the treatment of boundary conditions, and the meshing strategy could be found in Huang et al. (2005); Huang (2010), and Abdrabou et al. (2016).

3 Numerical and simulation results

3.1 RIB waveguide

In order to show the numerical precision of the proposed method, V-RCPSM, we studied a standard rib waveguide of silicon surrounded by air. The cross-section of the structure is shown in Fig. 2. The rib width, w is $3.0 \mu\text{m}$, the rib height, H , and the outer slab depth, D , is such that $H + D = 1 \mu\text{m}$, and the operating wavelength is $1.15 \mu\text{m}$. The refractive indices of the guiding, n_g , and substrate, n_s , regions are 3.44 and 3.4, respectively. Table 1 shows the values of the effective index of the fundamental mode H_{11}^y as the outer slab depth,

D , varies from 0.1 to $0.9 \mu m$, these being obtained by using our proposed full vectorial spectral method, V-RCPSM, and other vectorial formulations such as the full vector finite-element method (VFEM) with the results from Obayya et al. (2002). The results using this type of VFEM were calculated with a mesh of 5609 nodes, and the PML boundary condition is employed around the computational window. However, the results produced by our new spectral method, V-RCPSM, were calculated with a few basis functions in each region, 15 in the core and 10 in the cladding layers representing the degree of basis functions n Abdrabou et al. (2016) in each dimension and each domain, which produced a mesh of 3744 nodes (total number of unknowns) without any PML. As seen from Table 1, there is a very close agreement between the results from our new method V-RCPSM and other formulations.

Figure 3a shows the dominant field component H_x of the fundamental mode using our method. As clearly shown in Fig. 3b, the peaks of the non-dominant field component, H_y , around the dielectric corners reflect the accurate incorporation of the boundary condition at the interface between the different dielectric media.

Based on these promising results, we studied a 2D plasmonic waveguide and compared the results using FEM in the next example.

3.2 Plasmonic waveguide

To show the accuracy and the efficiency of our developed approach, V-RCPSM, we studied the conventional rectangular structure of the plasmonic waveguide introduced in Heikal et al. (2013) and shown in Fig. 4 with $w = 120nm$ and $d = 1200nm$. In this study, the refractive index of Gold is calculated using Johnson and Christy.

The following Table 2 shows the convergence study of the effective refractive index (n_{eff}) of the first TM Mode of the plasmonic waveguide shown in Fig. 2 at $1.5\mu m$ wavelength.

We found V-RCPSM converges at [38,38] basis functions for both the finite and semi-finite subdomains in the structure which produced 13689 unknowns leading to a characteristic matrix of size 27378. However, to get the same accuracy by the finite elements method (FEM) using the COMSOL software (Multiphysics 1998), we had to use two thin

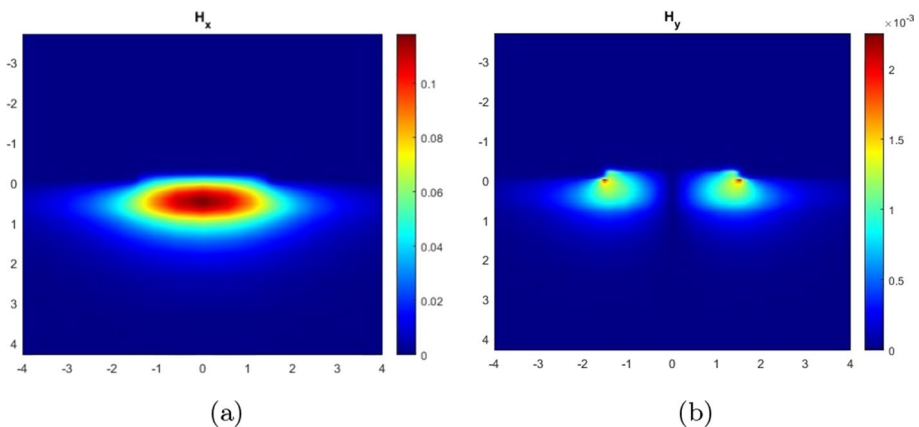


Fig. 3 (a) The dominant H_y field distribution and (b) the nondominant H_x field distribution for $D = 0.8\mu m$

Fig. 4 The 2D cross-section of a plasmonic waveguide

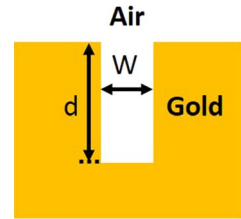


Table 2 V-RCPSM Convergence of the Effective Refractive Index (n_{eff}) of the First TM Mode at at $1.5\mu m$ wavelength

No. of basis function (N)	No. of the field unknowns	n_{eff}
8	1458	$1.057744476181819 + 0.011240457965115i$
18	6498	$1.125042139124131 + 0.009228057555147i$
28	15138	$1.131424295443487 + 0.008707870111658i$
30	17298	$1.131135043098768 + 0.008731365801020i$
34	22050	$1.132943134270351 + 0.008606970780766i$
36	24642	$1.133311770323560 + 0.008583578930814i$
38	27378	$1.133633745656570 + 0.008563436379935i$

Table 3 The number of elements produced by our code of V-RCPSM vs. FEM, the COMSOL software

	No of elements
FEM	740,528
V-RCPSM (Present)	27,377

layers of extra meshing around the interfaces between the metal and the dielectric material to be able to capture the correct rapid field variation there, the width of each layer was $1nm$ with a maximum element size of $0.2nm$ and a minimum element size of $0.1nm$. This extra meshing produces huge matrices with 740,528 elements and requires computational resources of 34.81 GB RAM during running FEM, COMSOL, for the 2D modal analysis at a single wavelength. Table 3 shows a comparison of the number of elements produced by our code of V-RCPSM vs. FEM, the COMSOL software.

In general, pseudo-spectral methods have a fast exponential convergence rate as noticed clearly from Table 2. And with a reasonable and small number of basis functions n , we can get very accurate results as shown in Sect. 3. As n increases very much, the convergence curve starts to diverge. That could happen because Chebyshev nodes are concentrated around the boundaries. So, when we use a small number of basis functions, the nodes concentrated at the boundaries will catch and represent the concentrated field there very well which is perfect for plasmonics. However, when we increase the number of basis functions too much, the Chebyshev nodes will be very very close to each other, and hence the linear system will become very ill-conditioned with very large condition number because of the singularity which may lead matrices with dependent/ or zeros rows or columns. Fortunately, the beauty of the pseudo-spectral Chebyshev method can produce very accurate results with just a few basis functions n thanks to its fast convergence rate, no need to increase n leading to ill-conditioned matrices.

Fig. 5 Real part of n_{eff} using the spectral method (V-RCPSM) and FEM while changing the wavelength (λ)

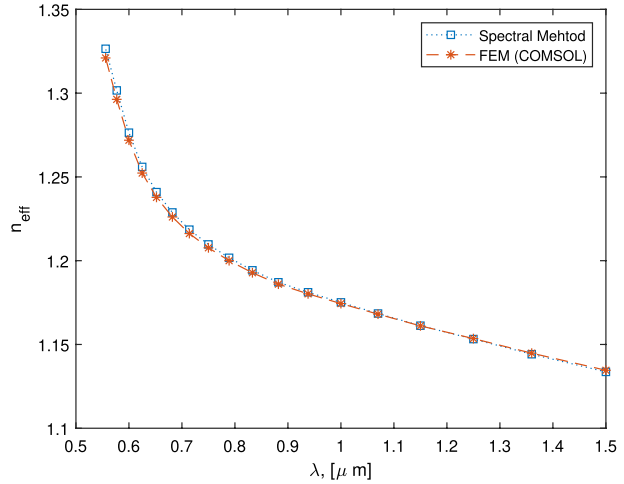
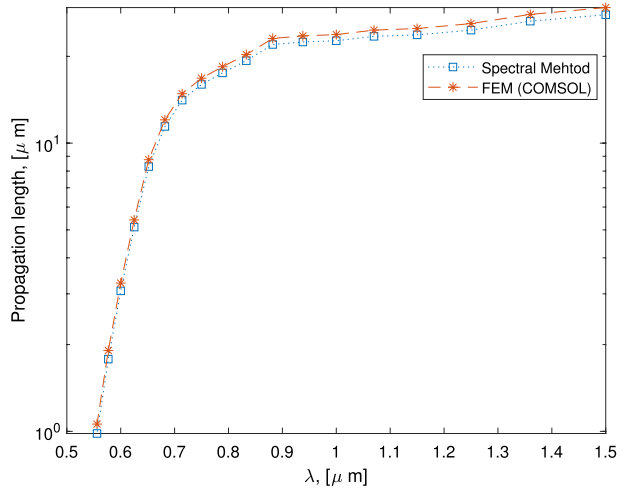
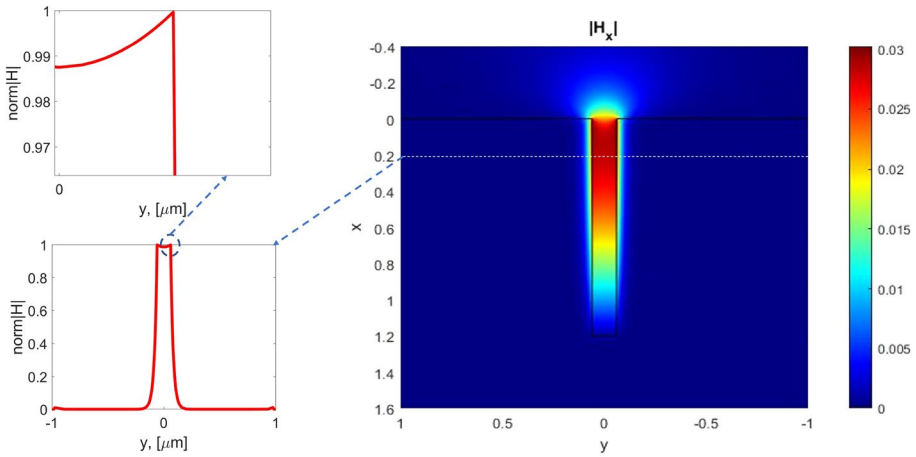


Fig. 6 Propagation length shown in log scale and calculated by $1/im(\beta)$ using the spectral method (V-RCPSM) and FEM while changing the wavelength

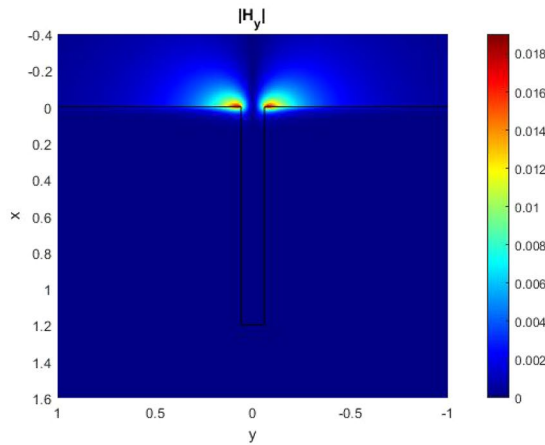


In Figs. 5 and 6, we compare n_{eff} and the propagation length, $1/im(\beta)$, obtained by the spectral method, V-RCPSM, with those obtained by the finite elements method (FEM) using the COMSOL software, respectively. Figure 7a and b show the dominant and minor components of the magnetic field, H_x and H_y , respectively, calculated by the spectral method, V-RCPSM, at $1.5\mu m$ wavelength. The insets of Fig. 7a show the great ability of the Rational Chebyshev functions to correctly capture the rapid variation and the sharp fields of the plasmonic mode at the interface between the metal and the dielectric material.

These results show great agreement between the FEM and the newly developed V-RCPSM. However, our V-RCPSM has achieved a great advantage over the FEM which is reducing the number of elements by 96% while getting the same accuracy as shown in Table 3.



(a)



(b)

Fig. 7 The absolute value of (a) the dominant component of the magnetic field, H_x , and (b) the minor component of the magnetic field, H_y , calculated by the presented method, V-RCPSM, at $1.5\mu\text{m}$ wavelength. The insets in (a) represent the norm magnetic field plotted at the cut-line of $x = 0.2\mu\text{m}$

4 Conclusion

The presented approach, V-RCPSM, was applied to the full-vectorial modal analysis of optical waveguides. The efficiency of our approach was demonstrated through the accurate calculation of the plasmonic and guided modes of two waveguides: the rib waveguide and the plasmonic waveguide. The adopted rational Chebyshev pseudo-spectral method captured the correct behavior of the sharp field at the high-index contrast interfaces of such waveguides and moreover yielded very good results with a number of basis functions less than that used by the conventional FEMs.

Acknowledgements The authors acknowledge the financial support by the Information Technology Industry Development Agency (ITIDA), Egypt, under Project ID: PRP2021.R30.13, and the technical support by Dr Amgad Abdrabou and Khaled Abo-Elsoud, an RA at Center for Photonics and Smart Materials.

Author contributions SO and AS have proposed the idea. AS has made the simulations and numerical results. All authors have contributed to the analysis, discussion, writing, and revision of the paper. SO has supervised the work done through the submitted manuscript.

Funding Open access funding provided by The Science, Technology & Innovation Funding Authority (STDF) in cooperation with The Egyptian Knowledge Bank (EKB). The authors acknowledge the financial support provided by the Information Technology Industry Development Agency (ITIDA), Egypt, under Project ID: PRP2021.R30.13

Data Availability The data will be available upon request.

Declarations

Conflict of interest The authors would like to clarify that there are no financial/non-financial interests that are directly or indirectly related to the work submitted for publication.

Ethical approval The authors declare no conflicts of interest related to this article.

Open Access This article is licensed under a Creative Commons Attribution 4.0 International License, which permits use, sharing, adaptation, distribution and reproduction in any medium or format, as long as you give appropriate credit to the original author(s) and the source, provide a link to the Creative Commons licence, and indicate if changes were made. The images or other third party material in this article are included in the article's Creative Commons licence, unless indicated otherwise in a credit line to the material. If material is not included in the article's Creative Commons licence and your intended use is not permitted by statutory regulation or exceeds the permitted use, you will need to obtain permission directly from the copyright holder. To view a copy of this licence, visit <http://creativecommons.org/licenses/by/4.0/>.

References

- Abdrabou, A., Heikal, A., Obayya, S.: Efficient rational chebyshev pseudo-spectral method with domain decomposition for optical waveguides modal analysis. *Opt. Express* **24**(10), 10495–10511 (2016)
- Atia, K.S., Said, A., Heikal, A., Obayya, S.: Compact and efficient 2d and 3d designs for photonic-to-plasmonic coupler. *JOSA B* **36**(6), 1402–1407 (2019)
- Azzam, S.I., Hameed, M.F.O., Shehata, R.E.A., Heikal, A., Obayya, S.S.: Multichannel photonic crystal fiber surface plasmon resonance based sensor. *Opt. Quant. Electron.* **48**, 1–11 (2016)
- Carvalho, F., W.O., Mejía-Salazar, J.R.: Plasmonics for telecommunications applications. *Sensors* **20**(9), 2488–2508 (2020)
- Gamal, Y., Younis, B., Hegazy, S.F., Badr, Y., Hameed, M.F.O., Obayya, S.: Highly sensitive multi-functional plasmonic biosensor based on dual core photonic crystal fiber. *IEEE Sens. J.* **22**(7), 6731–6738 (2022)
- Heikal, A.M., Hameed, M.F.O., Obayya, S.S.: Improved trenched channel plasmonic waveguide. *J. Lightwave Technol.* **31**(13), 2184–2191 (2013)
- Huang, C.-C.: Modeling mode characteristics of transverse anisotropic waveguides using a vector pseudospectral approach. *Opt. Express* **18**(25), 26583–26599 (2010)
- Huang, C.-C., Huang, C.-C., Yang, J.-Y.: A full-vectorial pseudospectral modal analysis of dielectric optical waveguides with stepped refractive index profiles. *IEEE J. Sel. Top. Quantum Electron.* **11**(2), 457–465 (2005)
- Koshiba, M., Tsuji, Y.: Curvilinear hybrid edge/nodal elements with triangular shape for guided-wave problems. *J. Lightwave Technol.* **18**(5), 737–743 (2000)
- Koshiba, M., Hayata, K., Suzuki, M.: Approximate scalar finite-element analysis of anisotropic optical waveguides. *Electron. Lett.* **10**(18), 411–413 (1982)
- Lager, I.E., Mur, G.: Generalized cartesian finite elements. *IEEE Trans. Magn.* **34**(4), 2220–2227 (1998)

- Lee, C., Lawrie, B., Pooser, R., Lee, K.-G., Rockstuhl, C., Tame, M.: Quantum plasmonic sensors. *Chem. Rev.* **121**(8), 4743–4804 (2021)
- Lusse, P., Stuwe, P., Schule, J., Unger, H.-G.: Analysis of vectorial mode fields in optical waveguides by a new finite difference method. *J. Lightw. Technol.* **12**(3), 487–494 (1994)
- Maier, S.A.: Plasmonics: the promise of highly integrated optical devices. *IEEE J. Sel. Top. Quantum Electron.* **12**(6), 1671–1677 (2006)
- Multiphysics, C.: Introduction to comsol multiphysics®. COMSOL Multiphysics, Burlington, MA, accessed Feb 9, 2018 (1998)
- Obayya, S., Rahman, B.A., Grattan, K.T., El-Mikati, H.: Full vectorial finite-element-based imaginary distance beam propagation solution of complex modes in optical waveguides. *J. Lightwave Technol.* **20**(6), 1054 (2002)
- Obayya, S., Somasiri, N., Rahman, B., Grattan, K.: Full vectorial finite element modeling of novel polarization rotators. *Opt. Quant. Electron.* **35**, 297–312 (2003)
- Ozbay, E.: Plasmonics: merging photonics and electronics at nanoscale dimensions. *Science* **311**(5758), 189–193 (2006)
- Said, A., Atia, K.S., Obayya, S.: On modeling of plasmonic devices: overview. *JOSA B* **37**(11), 163–174 (2020)

Publisher's Note Springer Nature remains neutral with regard to jurisdictional claims in published maps and institutional affiliations.